Soft Matter

PAPER

View Article Online
View Journal | View Issue

Cite this: *Soft Matter*, 2025, **21**, 504

Tunable mechanical properties of PDMS–TMPTMA microcapsules for controlled release in coatings†

Congwang Ye,[b] Bianka Pajo[a] and Carlos J. Martinez *[a]

Received 18th September 2024,
Accepted 14th December 2024

DOI: 10.1039/d4sm01107d

rsc.li/soft-matter-journal

Within coating formulations, microcapsules serve as vehicles for delivering compounds like catalysts and self-healing agents. Designing microcapsules with precise mechanical characteristics is crucial to ensure their contents' timely release and minimize residual shell fragments, thereby avoiding adverse impacts on the coating quality. With these constraints in mind, we explored the use of 1 cSt PDMS oil as a diluent (porogen) in trimethylolpropane trimethacrylate (TMPTMA)-based to fabricate microcapsules with customized mechanical properties and submicrometer debris size after shell breakup that can encapsulate a wide range of compounds. Microcapsules were fabricated from double emulsion templates featuring an aqueous core and shells with different PDMS : TMPTMA volume percent ratios. Their mechanical properties under compression and their capacity for encapsulation were characterized. PDMS : TMPTMA ratios exceeding 20 : 80 caused phase separation during crosslinking, leading to a porous shell structure of TMPTMA clusters. The strength of the microcapsules decreased as the PDMS:TMPTMA ratio increased, with ratios above 30 : 70 resulting in mechanically fragile microcapsules fracturing into fragments <10 μm in size. Microcapsules produced with a 0 : 100 PDMS : TMPTMA ratio exhibited strong mechanical properties and were capable of encapsulating small volatile compounds like 1,4-diazabicyclo[2.2.2]octane (a catalyst), while those with ratios $>30:70$ were only suitable to encapsulate larger molecules. The combination of PDMS:TMPTMA chemistry and the precise control provided by the double emulsion generation process in microcapillary devices makes PDMS:TMPTMA a versatile system suitable for various pressure-sensitive encapsulation applications.

1 Introduction

Microcapsules are used in a wide range of applications such as drug delivery,[1] organic phase change materials[2] and in coating formulations to control the release of additives and more recently for self-healing coating applications.[3–6] The efficacy of microcapsules in delivering its content depends on the ratio of the thickness of the shell to the capsule radius, as well as its material properties.[7–9] Advanced applications such as the delivery of catalysts in coatings require microcapsules with custom mechanical properties so that they are easily broken before or during the coating application process.[10–12] Furthermore, the fate of the residual shell material after breakage must be considered in the microcapsule design to ensure that it does not interfere with the aesthetics and properties of the coating. One approach is to fabricate microcapsules with sub-micrometer-thick shells and diameters significantly smaller than the coating thickness. However, in some cases, larger and thicker microcapsules are needed due to the chemistry of the encapsulated material or application requirements. Therefore, there is interest in finding shell chemistries that facilitate encapsulation and disintegrate under pressure.

Microcapsules can be fabricated using liquids and solids as templates. For example, Pickering and surfactant-stabilized single emulsions fabricated *via* shear-driven emulsification have been used to fabricate polymeric or ceramic microcapsules *via* interfacial polymerization.[13,14] Another approach is using particle templates coated with polyelectrolytes.[15–17] Both techniques yield microcapsules with highly elastic shells and thicknesses ranging from hundreds of nanometers to tens of micrometers. Microcapsules with thicker shells and a wider range of materials can be obtained from double emulsion drops generated in microfluidic devices.[18–20] Drops are generated by carefully tuning the dispersed and continuous phase flow rates to induce drop breakup in the dripping regime where their diameters are highly uniform.[10,18] Once the drops are generated, the fluid shells are solidified through crosslinking or polymerization.[21,22] Acrylates have gained popularity as shell materials in microfluidic double emulsion-based capsule generation due to their low viscosity, high reactivity, a wide range of chemistries, and ease of UV-crosslinking. Acrylates are usually used as the oil phase to form water/oil/water (w/o/w) double emulsion templates. For example, Chen *et al.*,[12,21]

[a] *School of Materials Engineering, Purdue University, 701 West Stadium Ave, West Lafayette, IN 47907, USA. E-mail: martin19@purdue.edu*
[b] *Materials Engineering Division, Lawrence Livermore National Lab, Livermore, CA 94550, USA*

† Electronic supplementary information (ESI) available. See DOI: https://doi.org/10.1039/d4sm01107d

successfully used silica-reinforced acrylates to encapsulate amines for self-healing applications. One modification to the acrylate composition that has not received much attention is the addition of diluents to form porous shells. Porous polymer particles and films can be obtained by adding a diluent such as acetone, toluene, or hexane. These porous particles belong to a class of microporous polymers formed due to the polymers' phase separation during crosslinking.[23] Macroporous polymers composed of styrene and divinyl benzene monomers have been extensively studied in the presence of solvating and non-solvating diluents and a wide range of crosslinker concentrations to form porous structures with tailored porous microstructures.[24] More recently, Loiseau *et al.*,[25] fabricated highly porous glycidyl methacrylate and ethylene glycol dimethacrylate microcapsules *via* double emulsion microfluidics. Mixtures of butanol and undecanol served as a diluent, forming porous shells composed of polymer aggregates similar to colloidosomes. The microcapsules' shell porosity was tailored by the amount and solubility of the diluent. Higher porosity decreased the shell strength and increased its permeability. Despite their high porosity, the capsules were stronger than similar colloidosome capsules. These results show that carefully introducing porosity to an otherwise strong polymer can be a novel route to control the mechanical properties of shells. Moreover, using a porous, brittle polymer can reduce the size of the residual shell material, which can be beneficial for coating applications. One of the main considerations in selecting the materials for tuning the microcapsule shells' porosity and mechanical properties is the polymer and diluent phase solubility parameters. Matching the solubility parameters between the materials is crucial to ensure phase separation between the two and, therefore, porosity and mechanical properties of the shell. According to Mohamed *et al.*,[26] if the diluent has good miscibility with the monomer and its polymeric form, it will result in a low pore volume. The opposite is true when the diluent is a bad solvent for the polymer phase, which results in the formation of macropores and an increase in polymer porosity.

In this work, we explore the use of 1 cSt PDMS oil as a diluent (porogen) in trimethylolpropane trimethacrylate (TMPTMA) with the aim of fabricating microcapsules with tailored mechanical properties and submicrometer residual shell size that can encapsulate a wide range of chemical compounds. TMPTMA is a highly reactive UV-cross-linkable methacrylate that is widely used as a strength modifier in acrylate-based formulations.[27–29] 1 cSt PDMS oil was chosen as the diluent (porogen) because of its ease of emulsification, non-reactivity with polar compounds, low viscosity, Newtonian behavior, and volatility.[30] Microcapsules with different PDMS: TMPTMA vol% ratios as the shell material were successfully fabricated from double emulsion drops generated in microcapillary devices. Soon after generation, the double emulsion drops were UV-crosslinked to solidify the shell, followed by harvesting from the solution and removal of the 1 cSt PDMS oil by evaporation. An in-house-built compression testing system was used to find the load to failure of hollow microcapsules with shells fabricated using different PDMS oil concentrations. The encapsulation capabilities of PDMS:TMPTMA microcapsules and the residual shell size after disintegration under pressure were also investigated.

2 Experimental setup

2.1 Materials

Three fluids, inner, middle, and outer, are needed to fabricate the double emulsions that served as precursors for the PDMS:TMPTMA microcapsules. Drop generation was tested using an aqueous solution (DI-H_2O) as the inner fluid while the middle fluid (shell) was composed of mixtures of octamethyltrisiloxane (1 cSt PDMS oil, Clearco Products, Bensalem, PA), trimethylolpropane trimethacrylate (TMPTMA, stabilized with hydroquinone monomethyl ether) (TCI, Tokyo, Japan) and photoinitator 2,2-dimethoxy-2-phenylacetophenone (Sigma, St. Louis, MO). The octamethyltrisiloxane will be referred to as PDMS through the document. Decamethylcyclopentasiloxane with trimethylated silicia (749 fluid, Dow Corning, Midland, MI) served as a surfactant and 2 wt% was added to all PDMS:TMPTMA mixtures. The outer fluid that served as the continuous phase was 40 wt% glycerol (99% (GC), Sigma, St. Louis, MO), 2 wt% poly(vinyl alcohol) (PVA) (M_w = 13 000–23 000 g mol^{-1}, 87–89% hydrolyzed, Sigma, St. Louis, MO) in DI-H_2O. The encapsulation capabilities of the solid and porous TMPTMA microcapsules were demonstrated using 1,4-diazabicyclo[2.2.2]octane (DABCO) (M_w = 112.17 g mol^{-1}), a catalyst used in coating formulations, resazurin dye (251.15 g mol^{-1}) (Sigma, St. Louis, MO) and fluorescein isothiocyanate–dextran (FITC–dextran) (M_w = 4000 g mol^{-1}) (Sigma, St. Louis, MO). Resazurin was chosen because of its intense purple color, which is easily seen by the naked eye. The viscosity of the PDMS:TMPTMA mixtures was measured using a rheometer (Gemini HR Nano, Malvern, Worcestershire, UK) using double-gap and concentric cylinder geometries.

2.2 Microcapillary devices

Microcapillary devices were fabricated following the work of Utada *et al.*,[18] and Shirk *et al.*[19] Briefly, two tapered round capillaries with 1 mm outer diameter were aligned and inserted in a square capillary of similar inner size, forming a coaxial structure suitable for double emulsion generation. A pipette puller (model P-97, Sutter Instruments, Novato, CA) was used to heat and pull the round glass capillaries (inner diameter: 0.580 mm, outer diameter: 1.000 mm, World Precision Instruments, Sarasota, FL) into two equal-sized tapered capillaries. A microforge station (Micro Forge MF830, Narishige, Japan) cleaved the tapered tips to the desired diameters. The surface of the input capillary was treated to be hydrophobic with a solution composed of 9.5 mL of 200-proof ethanol (KOPTEC, King of Prussia, PA) and 0.5 mL of chlorotrimethylsilane (Sigma, St. Louis, MO). The exit capillary was treated to be hydrophilic with a solution of 9.0 mL of 200 proof ethanol (KOPTEC, King of Prussia, PA), 0.5 mL of DI-H_2O, 0.1 mL of acetic acid (Sigma, St. Louis, MO) and 0.2 mL of 2-[methoxy(polyethyleneoxy)propyl]trimethoxysilane (Sigma, St. Louis, MO). Three 20G Luer stubs (Intramedic Luer Stub Adapters, Beckton Dickinson, Sparks, MD) were used as input connectors for the three fluids. Each opening was closed with marine epoxy

(Henkel, Rocky Hill, CT) and/or 5-minute epoxy (Permatex, Solon, OH), and the entire structure was fixed to a 6 x 2 inches glass slide.

2.3 Double emulsion generation and characterization

Double emulsions were generated by first loading the respective solutions into glass syringes (Hamilton Gastight, Hamilton Co., Reno, NV) controlled by syringe pumps (PHD 2000, Harvard Apparatus, Holliston, MA) and connected to microcapillary devices using polyethylene tubing (Smiths Medical ASD, Inc., Keene, NH). The drop generation was controlled by independently adjusting the flow rates of the inner (Q_{inn}), middle (Q_{mid}), and outer (Q_{out}) fluid and the process was visualized on an inverted microscope (Axio Observer, Zeiss America, Peabody, MA) equipped with a fast camera (Photron FASTCAM MINI UX100, Photron USA, Inc., San Diego, CA). The drops were irradiated with UV light (CE-6-BL, American Ultraviolet Co., Lebanon, IN) 10 seconds after generation to initiate shell crosslinking and reduce the diffusion of the inner fluid to the continuous phase due to an osmotic pressure gradient.[19] Microcapsules were collected in a partially filled vial with DI-H_2O, or in a funnel with filter paper to speed up the elimination and drying of the continuous phase. The collected microcapsules were rinsed with DI-H_2O and removed from the funnel while adhering to the filter paper, followed by an hour of UV post-curing to ensure complete crosslinking of the shells. The dried capsules were then collected in vials for storage.

An aliquot of the samples was collected in rectangular flat capillaries (Vitrocom, Mountain Lakes, NJ) with dimensions of 4 mm width, 0.4 mm height, and 55 mm length to optically visualize drops and microcapsules. The flat capillaries were glued to a glass slide, and the ends were covered with epoxy to reduce evaporation. Bright-field and fluorescence optical images were taken on an inverted microscope with a QICAM digital camera (QICAM 12-bit Cooled ColorFast 1394 Cooled, Qimaging, Surrey, BC, Canada). Optical images were analyzed using ImageJ (National Institutes of Health, Bethesda, MD) to measure the inner (d_{inn}) and outer (d_{out}) drop diameters. Dry microcapsules were placed on carbon tape fixed to an aluminum stub and sputter-coated with a 10-nm gold layer for SEM imaging (Phenom Pure, Phenom World, Eindhoven, The Netherlands).

2.4 Microcapsule compression testing

The load-to-failure and load–displacement curves for PDMS:TMPTMA microcapsules were measured using an "in-house" built compression apparatus inspired by the work of White *et al.*[31] The apparatus, containing a load cell and a motorized stage, was mounted on an inverted microscope as shown in Fig. S1 (ESI†). Several studies[1,2] on the mechanical properties of microcapsules with porous shells for controlled release of active components have reported applied loads on the 0–1000 mN range from compression tests performed on single capsules.[25] This study also chose such loads to evaluate the strength and mechanical properties of the PDMS:TMPTMA microcapsules. The microcapsules were compressed by a cylindrical stainless steel tapered tip connected to the load cell, and the motorized stage controlled the motion of the tip. Data were collected and displayed using LabView. The final load–displacement curve was obtained after subtracting the machine compliance. Capsule compression and subsequent rupture were recorded using the fast camera described above.

3 Results and discussion

3.1 Rheology of PDMS:TMPTMA solutions

PDMS oil readily mixed with TMPTMA at all concentrations without signs of phase separation. PDMS oil has a solubility parameter (δ_1) of $\sim$15(MPa)$^{1/2}$,[32,33] while the solubility parameter for TMPTMA (δ_2) is $\sim$18.3(MPa)$^{1/2}$.[34] The $\Delta\delta^2 = (\delta_1 - \delta_2)^2$ for the PDMS:TMPTMA solutions is 8.19 MPa making PDMS oil a good to moderate solvent for the TMPTMA monomer. On the other hand, $\Delta\delta^2$ between PDMS oil and crosslinked TMPTMA ($\delta \sim 23$ MPa$^{1/2}$) is $\sim$64 MPa, making PDMS oil a poor solvent for the TMPTMAs polymer and will result in an early phase separation between the two during UV crosslinking and as a result increasing the shell porosity. The behavior of the PDMS:TMPTMA solutions resembled that of a solvent/low molecular weight polymer mixture. To corroborate this, viscosity measurements were performed on solutions with different PDMS : TMPTMA vol% ratios, as shown in Fig. 1a. The apparent viscosity (η_{app}) as a function of shear rate ($\dot{\gamma}$) is Newtonian for all mixtures ranging from 0.00087 Pa s for 100 : 0 PDMS : TMPTMA ratio and 0.045 Pa s for a 0 : 100 PDMS : TMPTMA ratio. The Newtonian behavior of the mixtures suggests that the PDMS oil acts as a good solvent for the TMPTMA monomer. η_{app} for each solution at 10 s^{-1} was plotted as a function of PDMS : TMPTMA vol% ratio in Fig. 1b. The modified version of the Arrhenius rule of mixtures developed by Lederer[35,36] to predict the viscosity of crude oil and solvent mixtures fit the data well as shown by the dashed line in Fig. 1b. The general form of the Lederer equation is $\ln \eta_{12} = x_1 \ln \eta_1 + x_2 \ln \eta_2$, where η_{12} is the mixture viscosity, η_1 and η_2 are the viscosities of the two components and x_1 and x_2 are the modified volume fractions using $x_1 = \frac{\alpha V_1}{\alpha V_1 + V_2}$, $x_2 = 1 - x_1$ and $\alpha = \frac{\gamma}{\ln\left(\frac{\eta_1}{\eta_2}\right)}$, where γ is 2.5, based on Einstein's diffusion equation for infinitely diluted suspensions and molecules. The low viscosity across the whole range of PDMS : TMPTMA ratios ensures that the mixtures are suitable for generating drops in microfluidic devices because the pressure in the small channels will not be excessively high, which can lead to syringe pump stalling.

3.2 0 : 100 PDMS : TMPTMA microcapsule fabrication

Microcapsule fabrication was started using a 0 : 100 PDMS : TMPTMA ratio. The purpose of these experiments was to understand the properties of the TMPTMA microcapsule without PDMS oil and serve as a baseline for other mixtures. Fabrication starts with double emulsion drop generation in microcapillary devices. An optical image of the generation of double emulsion drops composed of an aqueous core surrounded by a 0 : 100 PDMS : TMPTMA shell near the entrance of the exit capillary is

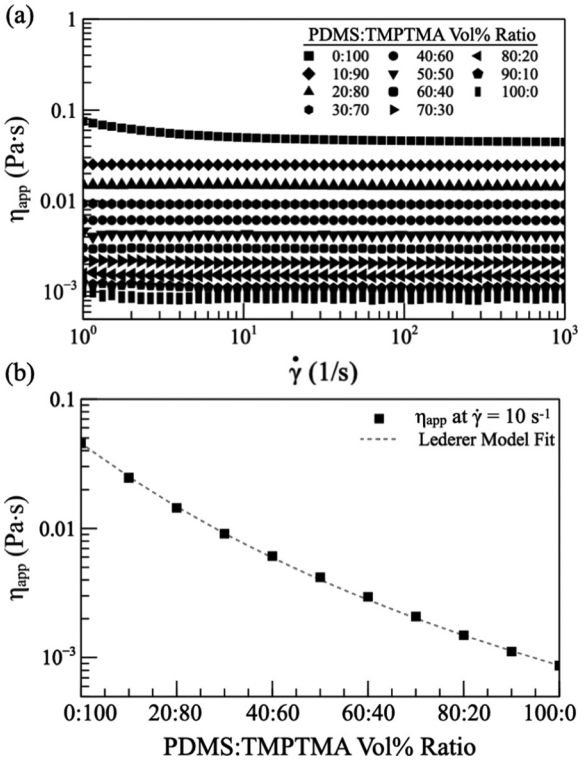

Fig. 1 (a) Apparent viscosity (η_{app}) as a function of shear rate ($\dot{\gamma}$) for solutions with different PDMS:TMPTMA vol% ratios. (b) η_{app} at $\dot{\gamma}$ = 10^{-1} s as a function of PDMS : TMPTMA vol% ratios.

shown in Fig. 2a. The inner (DI-H_2O) and middle (TMPTMA) fluids meet at the entrance of the exit capillary, where they are sheared by the outer aqueous fluid, breaking into double emulsion drops in a single step. Drop breakup occurs due to the interplay between viscous stress and interfacial tension between the fluids.[37,38] Double emulsion drops were exposed to UV light as they traversed the exit tubing to partially crosslink the TMPTMA shell and prevent inner drop breakup or coalescence. The partially crosslinked microcapsules were collected in a glass vial and exposed to UV light for another 30 minutes to crosslink the shell fully. The crosslinked aqueous core/TMPTMA shell microcapsules are highly uniform with a coefficient of variation (CV) $<3\%$ for d_{inn} and d_{out}. One of the benefits of using a flow-focusing microcapillary device is that the inner and outer drop diameters can be adjusted by independently changing the three-fluid flow rates. A series of drop generation experiments were performed in which the Q_{out} was fixed to 8000 μL h^{-1} and Q_{mid} = 1500 μL h^{-1}, while the Q_{inn} was varied from 600 to 2400 μL h^{-1}. A plot showing d_{inn} and d_{out} as a function of $Q_{inn}/(Q_{mid} + Q_{out})$ and the shell thickness/outer radius ratio (t_{shell}/r_{out}) is shown in Fig. 2f. When the Q_{inn} increased from 600 to 2400 μL h^{-1}, the d_{inn} value increased from 189 to 213 μm, while the d_{out} value decreased from 280 to 255 μm. t_{shell} decreased from 91 to 42 μm corresponding to a t_{shell}/r_{out} of 0.33 to 0.16. Optical images of a group of crosslinked TMPTMA microcapsules dispersed in DI-H_2O and generated with different outer diameters and shell thicknesses are shown in Fig. 2b–e. Note that while the microcapsules' shell thickness appears uniform in most of the optical images, they are not uniform along the z-axis

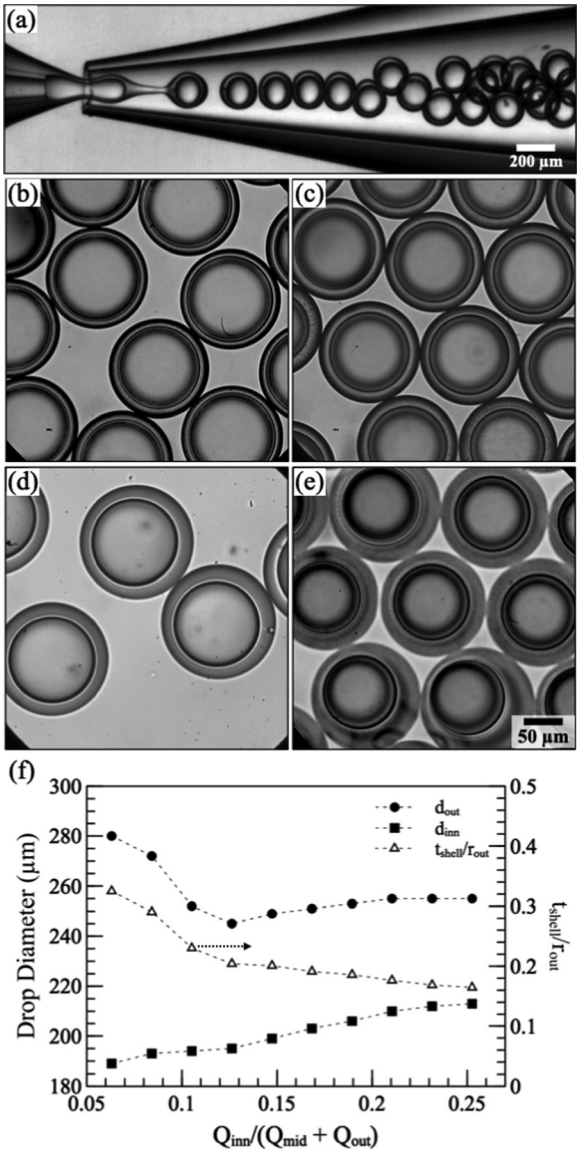

Fig. 2 Optical images showing the (a) generation of the DI-H_2O-core and 0 : 100 PDMS : TMPTMA vol% ratio shell double emulsion drops, and (b)–(e) group of collected double emulsion drops of similar composition with different shell thicknesses (t_{shell}). (f) Inner and outer drop diameters as well as the t_{shell} and outer radius (r_{out}) ratio as a function of the inner (Q_{inn}) and middle (Q_{mid}) plus outer (Q_{out}) flow rate ratio. The scale bar in (e) also applies to (b)–(d).

(gravitational axis) due to differences in the density between the aqueous core (ρ_{H_2O}= 1 g mL^{-1}) and the TMPTMA (ρ_{TMPTMA} = 1.06 g mL^{-1}) solution. The thinnest region of the shell is its weakest point, and it will influence the force at failure for microcapsules with similar shell thicknesses. Overall, the aqueous core/TMPTMA double emulsion drops are stable in solution, and due to the fast UV-crosslinking of the TMPTMA, $>98\%$ of the microcapsules survived the fabrication, crosslinking, and collection processes.

3.3 Mechanical properties of 0 : 100 PDMS : TMPTMA microcapsules

The fully crosslinked 0 : 100 PDMS : TMPTMA microcapsules were strong with a dense microstructure, as shown by the

partially broken capsules in Fig. 3(c and d). TMPTMA is known to be brittle and crack easily when cast on surfaces due to the residual stresses that develop during crosslinking.[39] TMPTMA microcapsules do not show cracks when viewed under a SEM or an optical microscope, except for those cracked intentionally during testing or for imaging purposes. This is due to the unconstrained nature of the drops, which allows the shell to shrink freely during crosslinking resulting in defect-free microcapsules. As previously discussed, the microcapsule shell thickness is not uniform due to the difference in density between the aqueous core and the TMPTMA shell, as can be seen in Fig. 3c and d. Attempts were made to obtain more uniform shell thicknesses by moving the UV light closer to the entrance of the exit capillary, where drops are generated. This resulted in device clogging due to premature TMPTMA crosslinking.

The strength of the microcapsules depends on the shell t_{shell}/r_{out} ratio, microstructure, outer diameter, and composition. For example, microcapsules with thick shells will be stronger than those with thinner ones.[21] The mechanical strength of 0 : 100 PDMS : TMPTMA microcapsules was assessed by evaluating the load displacement of microcapsules produced with varying t_{shell}/r_{out} ratios. Representative load *vs.* displacement curves of compression tests for microcapsules with a 0.169 t_{shell}/r_{out} ratio are shown in Fig. 3a. When the microcapsule cracks, there is a sudden decrease in the load due to their brittle nature. The load at failure increases with increasing t_{shell}/r_{out} as shown in Fig. 3b since a thicker shell can support the load over a large volume. The highest stress occurs at the compression contact poles, where the outer side of the shell is in compression while the inner side is in tension. The system's optics did not allow for a detailed image of the microcapsule surface before failure. However, high-speed video of the microcapsule-breaking process was captured, as shown in the sequence of images in Fig. S2 (ESI†), where the microcapsule appears as a black circle between two horizontal black regions corresponding to the compression tip and substrate. The microcapsule had a d_{inn} = 179 μm and d_{out} = 222 μm, corresponding to a t_{shell}/r_{out} = 0.096. The imposed load is dissipated once a crack starts propagating at high speed along the microcapsule in the longitudinal direction, shattering the shell into pieces seen as dark spots moving horizontally from the initial microcapsule location (Fig. S2, ESI†).

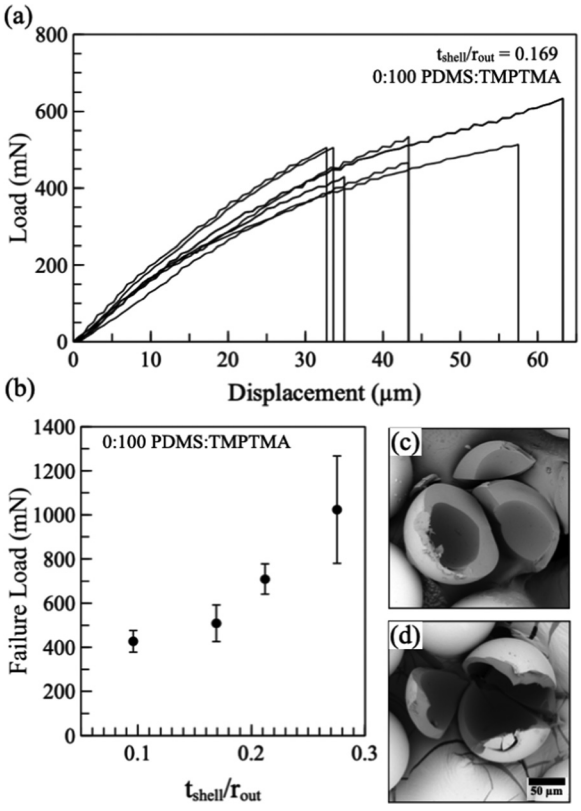

Fig. 3 (a) Load–displacement curves of compression tests for microcapsules made with 0 : 100 PDMS:TMPTMA mixture and a 0.169 t_{shell}/r_{out} ratio. (b) Failure load as a function of t_{shell}/r_{out}. (c) and (d) SEM images of acrylate capsules with different t_{shell}. Scale bar on (d) also applies to (c).

As t_{shell}/r_{out} increases, so does the measurement standard deviation, as shown in Fig. 3b. This is due to the random orientation of the thinnest part of the shell with respect to the applied load-axis, and this effect becomes more pronounced as t_{shell}/r_{out} increases. The lowest load to failure is expected if the thinnest region of the shell is aligned with the applied load axis.[21] Since the microcapsules are optically opaque, it is impossible to know the shell orientation; therefore higher variability is expected for microcapsules with thicker shells. As t_{shell}/r_{out} decreases, the microcapsules weaken, and the shell orientation effect diminishes.

Because of the microcapsule's brittle nature, their failure can be described using Weibull statistics. The probability of failure can be written as $P(F) = 1 - \exp[-(F_0/F)^m]$ where m is the Weibull modulus, and F_0 is the characteristics failure load. The Weibull modulus m can be obtained from the linear fit slope of the double logarithmic Weibull plot, while F_0 is the y-axis intercept. A summary of the Weibull statistics for the 0 : 100 PDMS : TMPTMA microcapsules is presented in Table 1. As the t_{shell}/r_{out} increases, F_0 increases from 448 to 1121 mN while m decreases from 9.4 to 4.4, indicating a higher variability in microcapsule strength distribution. The microcapsule modulus (M) also increased from 10 to 36.7 mN μm^{-1} with increasing t_{shell}/r_{out}. The findings indicate that the mechanical properties of 0 : 100 PDMS : TMPTMA microcapsules can be modified by altering the shell thickness. Significantly weaker microcapsules can be produced by reducing the TMPTMA shell thickness or outer diameter beyond the range explored in this study. Nevertheless, attempts to adjust the flow rates to make a thinner shell resulted in instability during the generation of double emulsion drops, and thus, this approach was not pursued further.

3.4 PDMS:TMPTMA microcapsule fabrication

Microcapsules with an aqueous core and different PDMS : TMPTMA ratios were generated in microcapillary devices from double emulsion drops containing increasing concentrations of 1cSt PDMS oil mixed with TMPTMA. Optical images of a group of UV-crosslinked capsules with DI-H_2O-cores and shells composed of (a) 10 : 90, (b) 20 : 80, (c) 30 : 70, and (d) 40 : 60

Table 1 Dimensions and mechanical property data of PDMS:TMPTMA microcapsule samples. t_{shell}/r_{out} is the shell thickness and outer radius ratio, F_0 is the characteristic Weibull load, m is the Weibull modulus, and M is the capsule modulus

PDMS : TMPTMA	d_{inn} (μm)	d_{out} (μm)	t_{shell}/r_{out}	M (mN μm^{-1})	m	F_0 (mN)
0 : 100	226	250	0.096	10	9.4	448.8
0 : 100	216	260	0.162	16.3	6.28	546.1
0 : 100	208	264	0.212	21.9	11.1	740.5
0 : 100	200	276	0.275	36.7	4.4	1121.5
0 : 100	150	181	0.171	4.98	6.40	145.9
10 : 90	154	187	0.176	4.94	8.19	139.5
20 : 80	158	191	0.173	4.79	14.3	119.97
30 : 70	182	220	0.173	4.53	2.09	92.7
40 : 60	185	229	0.192	2.55	4.16	12.78
50 : 50	199	248	0.198	1.58	4.70	4.85

PDMS : TMPTMA vol% ratios are shown in Fig. 4. The microcapsules were generated with similar d_{inn}, d_{out}, and t_{shell} by keeping a constant 1 : 1 rate Q_{mid}/Q_{inn} ratio and using the same microcapillary device. Double emulsions were stable, and the collected drops did not show signs of coalescence indicating that mixing PDMS oil with TMPTMA did not affect drop stability. Initially, all PDMS:TMPTMA solutions were optically clear, forming double emulsions with transparent cores and shells. As soon as the double emulsion drops were exposed to UV-light, the opacity of the shell increased with PDMS oil concentration, as shown in Fig. 4. The change in opacity is due to the difference in the refractive index between the PDMS oil and TMPTMA-crosslinked regions of the shell. A similar change in opacity has been reported in siloxane hydrogels containing a diluent phase.[40] Mixtures with up to 80 : 20 PDMS : TMPTMA vol% ratios were tested (not shown). However, microcapsules made with PDMS oil concentrations above 50 vol% were mechanically weak and broke easily during harvesting from solution, therefore were not mechanically tested.

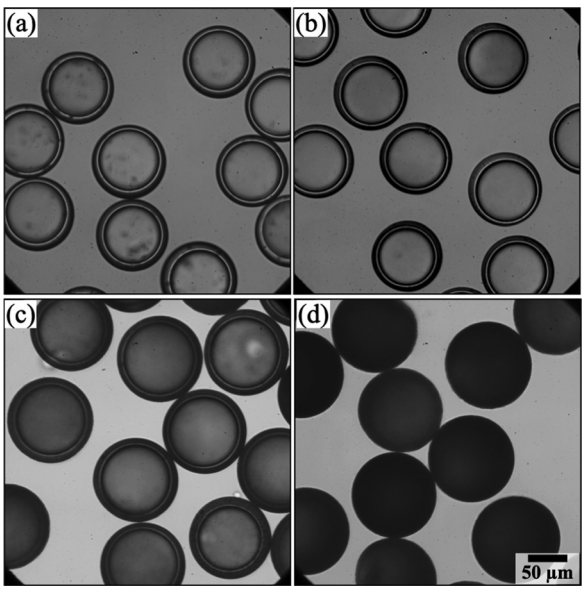

Fig. 4 Optical images of a group of UV-crosslinked capsules with DI-H_2O-cores and shells composed of (a) 10 : 90, (b) 20 : 80, (c) 30 : 70, and (d) 40 : 60 PDMS : TMPTMA vol% ratios. Scale bar in (d) applies to all images.

3.5 Mechanical properties of PDMS:TMPTMA microcapsules

Once generated, the PDMS:TMPTMA double emulsion drops were collected and fully UV-crosslinked for an additional 30 minutes. Microcapsules were harvested from the solution and dried for 24 hours under ambient conditions. During drying, the highly volatile 1 cSt PDMS oil evaporated from the shell leaving behind a porous microstructure composed of TMPTMA clusters as shown in Fig. 5c and d. Water also evaporated from the core. The porous structure is due to phase separation between the PDMS oil and

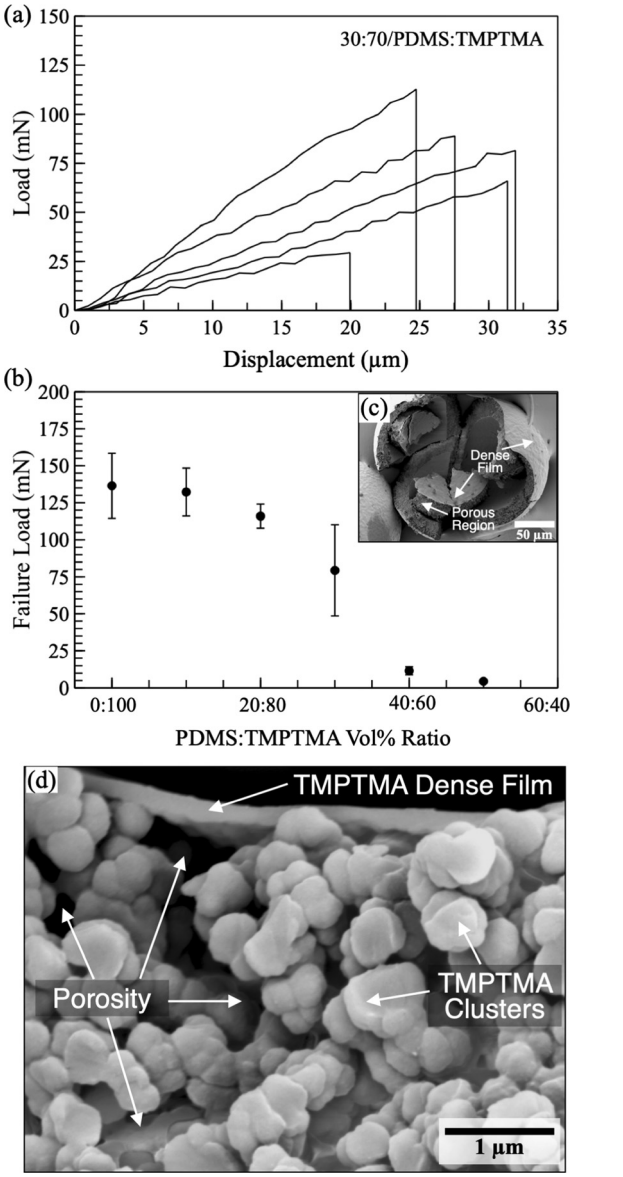

Fig. 5 (a) Load–displacement curves for microcapsules made with 30 : 70/PDMS : TMPTMA volume % ratio. (b) Failure load for microcapsules made with different PDMS : TMPTMA volume % ratios. SEM images of (c) a broken capsule fabricated with 30 : 70/PDMS : TMPTMA and (d) close-up of a section of the shell in (c), showing the TMPTMA clusters.

the TMPTMA during UV-crosslinking. Similar phase separation has been observed in fabricating thin films composed of TMPTMA and different solvents.[39,41,42] During UV-crosslinking of pure TMPTMA, nanoscale nucleation sites form, quickly growing and coalescing into a dense structure. When PDMS oil is added, the TMPTMA nucleation growth is suppressed, forming an interconnected network of TMPTMA particle aggregates. Porosity increases with PDMS oil concentration while the shell strength decreases. A close-up of a region of the shell showing the TMPTMA clusters is shown in Fig. 5d. The microstructure shown in Fig. 5d shows a higher porosity compared to the dense and microscale-pore-free microstructure shown in Fig. 3c and d for the 0 : 100 PDMS : TMPTMA microcapsules. Similar porosity has been reported for other polymer diluent mixtures.[25,26]

A dense polymer layer with a thickness between 200 and 300 nm covered both the inner and outer surfaces of the shell for samples with PDMS : TMPTMA ratios above 30 : 70 as shown in Fig. 5c and d. These dense, thin films have been previously reported and attributed to the presence of a poor solvent such as water.[43] Work by Davidson *et al.*[44] on polyvinyl chloride (PVC) particles showed that this type of skin layer is formed by adsorption and grafting of the agglomerated molecules at the interface.[45] The TMPTMA monomers nucleate near the poor solvent interface that rapidly coalesce into a thin film, correlating to the roughness observed in the inner surface of the skin layer (see Fig. 5d). As shown later, these dense TMPTMA layers help to encapsulate molecules that would otherwise permeate through the porous TMPTMA shell.

The load–displacement curves for the compression test of representative 30 : 70 PDMS : TMPTMA ratio microcapsules are shown in Fig. 5a. Note that the curves appear more linear than the 0 : 100 PDMS : TMPTMA microcapsules shown in Fig. 4a. The failure load *vs.* PDMS : TMPTMA vol% ratios are shown in Fig. 5b. As the PDMS : TMPTMA ratio increases, the failure load decreases, ranging from 0.138 N for microcapsules with a 0 : 100 PDMS : TMPTMA ratio to 0.004 N for those with a 50 : 50 ratio. The reduction in strength stems from increased shell porosity and the aggregated nature of the TMPTMA clusters. The load to failure decreases slightly for microcapsules made with $<30:70$ PDMS : TMPTMA ratios, while a significant reduction is observed for higher ratios. This trend can also be observed in both F_0 and M for the TMPTMA samples, as shown in Table 1. For example, M decreases moderately from 4.98 to 4.53 mN μm^{-1} for microcapsules with ratios less than 30 : 70, but a notable drop to 1.58 is seen when a 50 : 50 ratio is used. Similarly, F_0 declines from 145.9 mN at a 0 : 100 ratio to 4.85 mN at a 50 : 50 ratio. Like the 0 : 100 PDMS : TMPTMA only microcapsules, there is high variability in the failure load measurements due to the inhomogeneous thickness of the microcapsules and porosity. Samples made with 40 : 60 and 50 : 50 PDMS : TMPTMA ratios show a narrower standard deviation in the load to failure since their shell microstructure is too weak to support the applied load, and the shell orientation becomes less relevant. Furthermore, the sensitivity of the load sensor is insufficient. The wide distribution of the shell strength results in low values of m ranging from 14.3 to 2.09 (see Table 1). In practical terms, using a PDMS : TMPTMA ratio greater than 30 : 70 for the fabrication of dry microcapsules is not recommended, as these microcapsules may lack the necessary strength to survive processing and drying. Nevertheless, microcapsules with ratios exceeding 30 : 70 can be utilized if they are maintained in suspension under low shear conditions.

3.6 Microcapsules encapsulation efficiency

While this work focused on tailoring the mechanical properties of TMPTMA microcapsules, their encapsulation efficiency was also evaluated, but not exhaustively. Testing started with resazurin (M_w = 251 g mol^{-1}), a dye with weak fluorescence used in biology that has an intense purple/blue color in aqueous solutions, so leakage from the microcapsules can be seen with the naked eye. Non-porous 0 : 100 PDMS : TMPTMA microcapsules were prepared with a 10^{-3} M resazurin aqueous solution in the core as shown in Fig. 6(a). In the initial encapsulation experiments, considerable leakage occurred from the double emulsion droplets prior to UV-crosslinking as they traveled through the collection tubing. It appeared that diffusion through the TMPTMA shell was the main cause of the resazurin leakage and crosslinking should be done as soon as the drops are generated. Hence, the UV light was moved to a distance of approximately 10 cm from the drop formation location within the microcapillary devices, ensuring it wasn't so close as to cause early crosslinking and clogging of the microcapillary device. Following these adjustments, the encapsulation efficiency improved, and the sole cause of resazurin leakage was due to the occasional breakup of the inner drops before crosslinking. Furthermore, the resazurin aqueous solution was successfully encapsulated in UV-crosslinked 60 : 40 PDMS : TMPTMA microcapsules as shown in Fig. 6c where the shell has a white appearance while the resazurin core is purple. 60 : 40 PDMS : TMPTMA microcapsules required gentle cleaning and postprocessing to prevent breakup since they were fragile, but we estimate that $>90\%$ survived when left in solution after cleaning. On a different test, a 10^{-3} M FITC–dextran (M_w = 4000 g mol^{-1}) aqueous solution was successfully encapsulated in 0 : 100 PDMS : TMPTMA microcapsules. The fluorescence intensity of the microcapsules was similar over a span of two months when stored in solution and covered to prevent FITC bleaching, as shown in Fig. 6d and e. Microcapsules with a PDMS : TMPTMA ratio greater than 0 : 100 and containing an aqueous FITC–dextran solution in the core were not produced due to the porous shell structure, which impeded fluorescence imaging. However, successful encapsulation is anticipated due to the higher molecular weight of FITC–dextran, which impedes diffusion through the shell regardless of its PDMS-oil content. Additionally, UV cross-linking could be performed after collection as the double emulsion drops were stable in the solution.

The encapsulation of DABCO, a commonly used catalyst, was also investigated and presented challenges not encountered with resazurin and PEG-dextran. DABCO has a molecular weight of 112.17 g mol^{-1} and is volatile under ambient conditions.[46] As noted earlier, water evaporates through the PDMS : TMPTMA

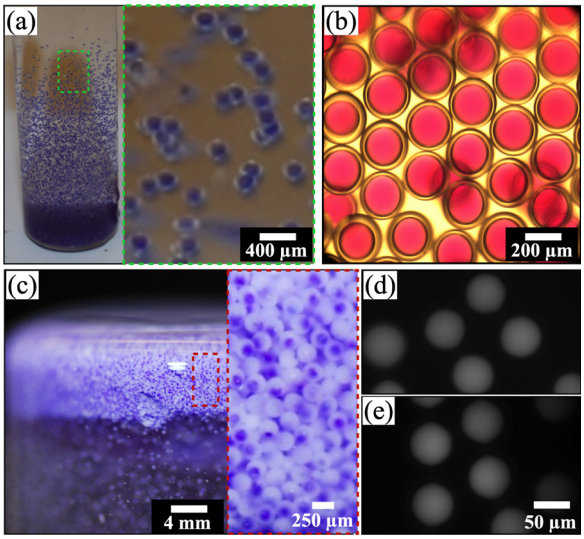

Fig. 6 Images of UV-crosslinked microcapsules featuring a core of aqueous rezasurin dye solution (purple) and shells made from (a) and (b) 0 : 100 and (c) 60 : 40 PDMS : TMPTMA vol% ratios. Fluorescence optical microscopy images show a cluster of microcapsules with aqueous FITC–dextran (M_w = 4000 g mol^{-1}) fluorescence cores and 0 : 100 PDMS : TMPTMA vol% ratio shells dispersed in water (d) 2 hours post UV-crosslinking and cleaning, and (e) 2 months later. The scale bar in (e) also applies to (d).

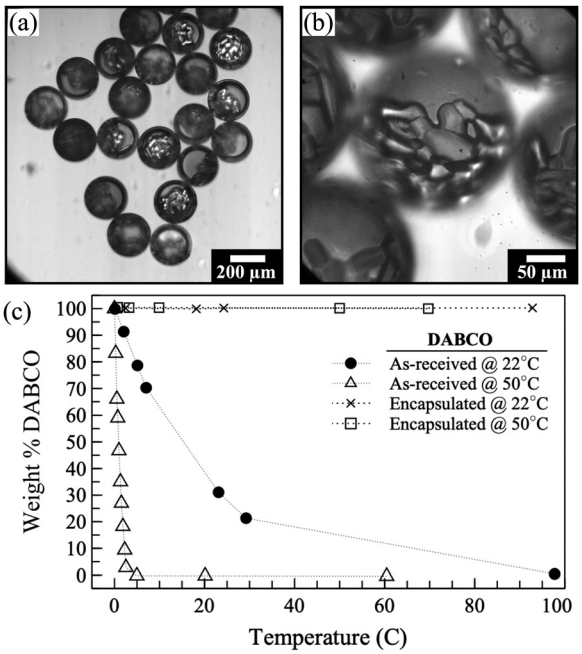

Fig. 7 (a) and (b) Optical images of dried 0 : 100 PDMS : TMPTMA vol% ratio microcapsules with DABCO precipitated in the core. (c) Weight % of the as-received and encapsulated DABCO at 22 and 50 °C as a function of time.

shells at all vol% ratios. Due to the volatile nature of DABCO, the objective was to assess if the microcapsules could prevent its evaporation. The testing started by fabricating microcapsules with 0 : 100 PDMS : TMPTMA shells and 0.2 g mL^{-1} aqueous DABCO solution in the core. Like with resazurin, it was essential to position the UV light near the drop-generation area in the microcapillary devices to prevent DABCO diffusion out of the double emulsion drops. After making these changes, DABCO was successfully encapsulated in 0 : 100 PDMS : TMPTMA microcapsules and, during drying, the water evaporated from the core and DABCO precipitated, as shown in Fig. 7a. Since the pH of the DABCO aqueous solutions changes with concentration, a calibration curve was measured as shown in Fig. S3 (ESI†) and this was used to estimate the remaining amount of DABCO in the microcapsules from pH measurements. A solution series was prepared with 0.257 g of crushed dried microcapsules mixed with 10 mL of DI-H_2O. If DABCO did not leak or evaporate from the microcapsules, the concentration of the crushed microcapsule DABCO solution should be 0.004 g mL^{-1} at a pH = 10.37, according to the calibration graph shown in Fig. S3 (ESI†). A pH of 10.33 ± 0.2 was measured, which corresponds to a DABCO concentration of 0.0035 g mL^{-1}, which means that 93% by weight of the initial DABCO concentration remained in the 0 : 100 PDMS : TMPTMA microcapsules. Furthermore, the microcapsules could encapsulate DABCO even at higher temperatures, as shown in Fig. 7c. In these experiments, the weight of 10 g of TMPTMA microcapsules was monitored at 22 °C and 50 °C for up to 100 hours and compared to non-encapsulated DABCO samples. The initial DABCO weight for the non-encapsulated samples was 1.32 g to match the DABCO weight inside the microcapsules. The weight% of non-encapsulated DABCO at 22 °C decreases with time due to evaporation, and the rate increases at 50 °C. The mass of the microcapsules remained constant over time, indicating their high efficiency in encapsulating DABCO.

Comparable pH DABCO experiments were conducted using porous microcapsules composed of 40 : 60 PDMS : TMPTMA, initially containing a 0.2 g mL^{-1} aqueous DABCO solution in their core. A series of solutions were prepared with 0.146 g of crushed dried microcapsules mixed with 10 mL of DI-H_2O. The pH of the solutions was 9.87 ± 0.3, corresponding to a DABCO concentration of 0.0001 g mL^{-1} or 20% by weight of the initial DABCO concentration that remained in the microcapsules. It seems that the leakage of DABCO was mainly due to evaporation through the shell during drying since some crude pH measurements in the solution indicate that the initial encapsulation was successful; however, more research is needed to corroborate this. Since 40 : 60 PDMS : TMPTMA microcapsules are opaque, no visual conformation of encapsulation was possible. These results suggest that porous microcapsules made using ratios >30 : 70 PDMS : TMPTA are ineffective at encapsulating low-molecular-weight volatile molecules such as DABCO but can effectively encapsulate chemicals with higher molecular weights. A more comprehensive study is needed to understand the effects of shell porosity on DABCO or a similar volatile molecule from PDMS:TMPTMA microcapsules.

A potential advantage of porous shells is that they break into smaller fragments than nonporous ones. A series of experiments were conducted to quantify the difference in the size of the shell fragments between porous 40 : 60 and 0 : 100 PDMS : TMPTA microcapsules with a nominal shell thickness of ≈24 μm. Ten grams of each microcapsule were crushed in a

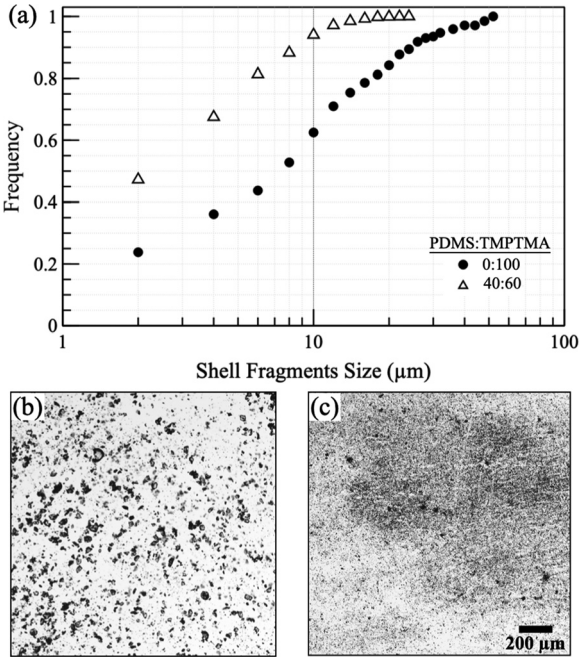

Fig. 8 (a) Relative frequency for the shell fragments left behind after microcapsules made with 0 and 40 vol% 1 cSt PDMS oil in TMPTMA which were manually crushed. Optical images of the shell fragments corresponding to crushed microcapsules fabricated with (b) 0 and (c) 40 vol% 1 cSt PDMS oil in TMPTMA solutions. The scale bar in (c) also applies to (b).

mortar and pestle for 1 minute followed by optical imaging to digitally measure the size of the shell fragments according to their Feret diameter. Fig. 8 illustrates the cumulative size distribution of the crushed shell fragments, indicating that the 40 : 60 PDMS : TMPTMA sample exhibits a smaller fragment size distribution than the 0 : 100 PDMS : TMPTMA sample. For example, the arithmetic mean fragment sizes are 4.5 μm for the 40 : 60 PDMS : TMPTMA and 11.4 μm for 0 : 100 PDMS : TMPTMA. Measurements coincide well with the visual size differences between the two samples as shown in Fig. 8b and c. These findings are anticipated because porous microcapsules are considerably less robust than their nonporous counterparts and can be broken with less force, as demonstrated in Fig. 5. The cumulative size data are limited by the resolving power of the 40× objective. Furthermore, reducing the fragment size of the 0 : 100 PMDS : TMPTMA sample could be achieved by increasing the crushing force, extending the crushing duration, or reducing the thickness of the shell. More detailed investigation is required to clarify the impact of these variables on the size of the shell fragment.

4 Conclusions

Microcapsules with varying PDMS : TMPTMA ratios were successfully fabricated from double emulsion droplets produced in microcapillary devices. The strength of the microcapsules diminished as the PDMS : TMPTMA vol % ratio increased, acting as a porogen during the UV-crosslinking of the shell. Microcapsules with a 0 : 100 PDMS : TMPTMA ratio exhibited no microscale porosity, were the most robust, and could encapsulate a low molecular weight volatile molecule such as DABCO. In contrast, microcapsules with PDMS : TMPTMA ratios exceeding 30 : 70 were mechanically weak and failed to encapsulate such molecules, but could encapsulate non-volatile molecules such as resazurin and FITC–dextran. Also, the shell fragment size was smaller for 40 : 60 PDMS:TMPTMA microcapsules than 0 : 100 PDMS : TMPTMA ones.

The PDMS : TMPTMA system offers flexibility when designing and making microcapsules *via* double emulsion generation. Drop generation was stable for hours and grams of microcapsules were produced daily and production can be scaled up using a multi-nozzle microcapillary/microfluidic arrangment. It is possible to not only tailor the mechanical properties by mixing PDMS oil and TMPTMA, but also, the microcapillary setup permits the control of microcapsule diameter and shell thickness by adjusting the middle and inner fluid flow rates. If strong microcapsules are desired, then a mixture with a $<30:70$ PDMS : TMPTMA ratio should be used. A $>30:70$ PDMS : TMPTMA ratio works well when weaker microcapsules are needed in solution. Overall, the PDMS:TMPTMA chemistry combined with the exquisite control over the double emulsion generation process in microcapillary devices offers a robust system that could be used in a wide range of pressure-sensitive encapsulation applications.

Author contributions

Congwang Ye – conceptualization, investigation, data curation, writing original draft, and writing review and editing. Bianka Pajo – data curation and writing review and editing. Carlos J. Martinez – funding acquisition, conceptualization, project administration, supervision, data curation, and writing review and editing.

Data availability

Data for this article, including Excel datasets, optical images, and videos, are available at **https://osf.io/vxqkh**.

Conflicts of interest

There are no conflicts to declare.

Acknowledgements

The authors wish to acknowledge the PPG corporation for their financial and technical support. Special thanks to David Walters and Dr. Scott Moravek for their invaluable technical guidance.

References

1 R. Kurapati, T. W. Groth and A. M. Raichur, *ACS Appl. Bio Mater.*, 2019, **2**, 5512–5527.
2 Y. Yoo, C. Martinez and J. P. Youngblood, *ACS Appl. Mater. Interfaces*, 2017, **9**, 31763–31776.
3 E. Koh, N.-K. Kim, J. Shin and Y.-W. Kim, *RSC Adv.*, 2014, **4**, 16214–16223.

4 T. Szabó, L. Molnár-Nagy, J. Bognár, L. Nyikos and J. Telegdi, *Prog. Org. Coat.*, 2011, **72**, 52–57.
5 T. Nesterova, K. Dam-Johansen and S. Kiil, *Prog. Org. Coat.*, 2011, **70**, 342–352.
6 M. A. Trojer, L. Nordstierna, J. Bergek, H. Blanck, K. Holmberg and M. Nyden, *Adv. Colloid Interface Sci.*, 2015, **222**, 18–43.
7 S. S. Bansode, S. K. Banarjee, D. D. Gaikwad, S. L. Jadhav and R. M. Thorat, *Int. J. Pharm. Sci. Rev. Res.*, 2010, **1**, 38–43.
8 F. Cárdenas-Bailón, G. Osorio-Revilla and T. Gallardo-Velázquez, *J. Microencapsulation*, 2013, **30**, 409–424.
9 Y. Li, L. Ai, W. Yokoyama, C. F. Shoemaker, D. Wei, J. Ma and F. Zhong, *J. Agric. Food Chem.*, 2013, **61**, 3311–3319.
10 P. W. Chen, R. M. Erb and A. R. Studart, *Langmuir*, 2012, **28**, 144–152.
11 M. W. Keller and N. R. Sottos, *Exp. Mech.*, 2006, **46**, 725–733.
12 P. W. Chen, G. Cadisch and A. R. Studart, *Langmuir*, 2014, **30**, 2346–2350.
13 J. O. Zoppe, R. A. Venditti and O. J. Rojas, *J. Colloid Interface Sci.*, 2012, **369**, 202–209.
14 M. Kobašlija and D. T. McQuade, *Macromolecules*, 2006, **39**, 6371–6375.
15 A. P. Johnston, C. Cortez, A. S. Angelatos and F. Caruso, *Curr. Opin. Colloid Interface Sci.*, 2006, **11**, 203–209.
16 C. J. Martinez, B. Hockey, C. B. Montgomery and S. Semancik, *Langmuir*, 2005, **21**, 7937–7944.
17 F. Caruso, R. A. Caruso and H. Mohwald, *Science*, 1998, **282**, 1111–1114.
18 A. S. Utada, E. Lorenceau, D. R. Link, P. D. Kaplan, H. A. Stone and D. A. Weitz, *Science*, 2005, **308**, 537–541.
19 K. Shirk, C. Steiner, J. W. Kim, M. Marquez and C. J. Martinez, *Langmuir*, 2013, **29**, 11849–11857.
20 C. Ye, A. Chen, P. Colombo and C. Martinez, *J. R. Soc., Interface*, 2010, **7**, S461–S473.
21 P. W. Chen, J. Brignoli and A. R. Studart, *Polymer*, 2014, **55**, 6837–6843.
22 R. K. Shah, H. C. Shum, A. C. Rowat, D. Lee, J. J. Agresti, A. S. Utada and L.-Y. Chu, *et al.*, *Mater. Today*, 2008, **11**, 18–27.
23 O. Okay, *Prog. Polym. Sci.*, 2000, **25**, 711–779.
24 W. L. Sederel and G. J. De Jong, *J. Appl. Polym. Sci.*, 1973, **17**, 2835–2846.
25 E. Loiseau, F. Niedermair, G. Albrecht, M. Frey, A. Hauser, P. A. Rühs and A. R. Studart, *Langmuir*, 2017, **33**, 2402–2410.
26 M. H. Mohamed and L. D. Wilson, *Nanomaterials*, 2012, **2**, 163–186.
27 N. Z. Noriman, H. Ismail, C. T. Ratnam and A. A. Rashid, *Polym.-Plast. Technol. Eng.*, 2010, **49**, 228–236.
28 D. S. Kim and W. H. Seo, *J. Appl. Polym. Sci.*, 2004, **92**, 3921–3928.
29 S. K. Datta, A. K. Bhowmick, T. K. Chaki, A. B. Majali and R. S. Despande, *Polymer*, 1996, **37**, 45–55.
30 R. Zivojnovic, *Silicone oil in vitreoretinal surgery*, Springer Science & Business Media, 2012, vol. 12.
31 J. D. Rule, N. R. Sottos and S. R. White, *Polymer*, 2007, **48**, 3520–3529.
32 M. Roth, *J. Polym. Sci., Part B: Polym. Phys.*, 1990, **28**, 2715–2719.
33 H. Yang, Q. T. Nguyen, Y. Ding, Y. Long and Z. Ping, *J. Membr. Sci.*, 2000, **164**, 37–43.
34 P. D. Drumheller and J. A. Hubbell, *J. Polym. Sci., Part A: Polym. Chem.*, 1994, **32**, 2715–2725.
35 E. L. Lederer, *Proc. World Pet. Cong. London*, 1933, **2**, 526–528.
36 W. R. Shu, *Soc. Pet. Eng. J.*, 1984, **24**, 277–282.
37 B. Ambravaneswaran, H. J. Subramani, S. D. Phillips and O. A. Basaran, *Phys. Rev. Lett.*, 2004, **93**, 034501.
38 C. Clanet and J. C. Lasheras, *J. Fluid Mech.*, 1999, **383**, 307–326.
39 C. Viklund, E. Pontén, B. Glad, K. Irgum, P. Hörstedt and F. Svec, *Chem. Mater.*, 1997, **9**, 463–471.
40 P. C. Nicolson and J. Vogt, *Biomaterials*, 2001, **22**, 3273–3283.
41 J. E. Rosenberg and P. Flodin, *Macromolecules*, 1986, **19**, 1543–1546.
42 A. Schmid and P. Flodin, *Die Makromol. Chem.*, 1992, **193**, 1579–1589.
43 P. Reinholdsson, T. Hargitai, R. Isaksson and B. Törnell, *Angew. Makromol. Chem.*, 1991, **192**, 113–132.
44 J. A. Davidson and D. E. Witenhafer, *J. Polym. Sci., Polym. Phys. Ed.*, 1980, **18**, 51–69.
45 B. Törnell and J. Uustalu, *J. Appl. Polym. Sci.*, 1988, **35**, 63–74.
46 A. Strachota, B. Strachotová and M. Šprková, *Mater. Manuf. Processes*, 2008, **23**, 566–570.